Temperature Dependence of Evaporation Coefficient for Water Measured in Droplets in Nitrogen under Atmospheric Pressure

D. JAKUBCZYK, M. ZIENTARA, K. KOLWAS, AND M. KOLWAS

Institute of Physics, Polish Academy of Sciences, Warsaw, Poland

(Manuscript received 26 January 2006, in final form 26 June 2006)

ABSTRACT

The evaporation and the thermal accommodation coefficients for water in nitrogen were investigated by means of the analysis of evaporation of pure water droplet as a function of temperature. The droplet was levitated in an electrodynamic trap placed in a climatic chamber. The levitation time was in the range of seconds, which corresponds to the characteristic time scales of cloud droplet growth. Droplet radius evolution and evaporation dynamics were studied as a function of temperature, by analyzing the angle-resolved light scattering Mie interference patterns. A model of droplet evolution, accounting for the kinetic effects near the droplet surface, was applied. The evaporation coefficient for the temperature range from 273.6 to 298.3 K was found to be between 0.054 and 0.12 with a minimum of 0.036 ± 0.015 seemingly coinciding with water maximum density at 277.1 K. The average value of thermal accommodation coefficient over the temperature range from 277 to 289 K was found to be 0.7 ± 0.2.

1. Introduction

The processes of evaporation and condensation are at the very heart of many fields of science. Cloud and aerosol microphysics together with construction of climate models (e.g., McFiggans et al. 2005; Laaksonen et al. 2004; Ackerman et al. 1995), electrospraying (e.g., Grimm and Beauchamp 2002), and combustion (e.g., Sazhin 2005) are just some areas of relevance. These processes are typically modeled with diffusion type mass and heat transport equations. Such models (originating from Maxwell) assume that space around a droplet is filled with gas and vapor in continuous way, and that an analogous assumption applies to temperature. In many cases, small droplets of size comparable to the mean free path of surrounding gas molecules are of interest, for example, in modeling cloud droplet growth (e.g., Laaksonen et al. 2004; Ackerman et al. 1995). Studying the evolution of droplets of such size requires analyzing the process in microscale and accounting for the kinetic effects. It is then necessary to supplement the diffusion coefficient, appearing in transport equations, with a so-called evaporation (condensation) or mass accommodation coefficient α_C. Likewise the thermal conductivity coefficient must be supplemented with a thermal accommodation coefficient α_T. These phenomenological coefficients describe the transport properties of the liquid–gas interface and are expected to describe only the properties of the very interface. All other processes influencing mass and heat transport, such as chemistry of the interface or the electrostatic interactions should be accounted for separately (Shi et al. 1999). The condensation coefficient α_C can be perceived as the probability that a vapor molecule (water in this case) impinging on the interface from the gaseous phase side enters into the bulk liquid and does not rebound. Similarly, the thermal accommodation coefficient α_T may be perceived as the probability of thermalization of the gas molecule (nitrogen or water vapor in this case) impinging the interface. It is often assumed that the evaporation and condensation coefficients are equal, which may not be the case (Marek and Straub 2001). It is also agreed, that α_C and α_T might possibly exhibit some temperature and pressure dependence (Marek and Straub 2001; Davidovits et al. 2004).

Since the values of α_C and α_T influence the rate of growth of droplets (growth time) at the early stage of the growth process, it also indirectly has some impact upon calculated relative humidity in the nascent cloud,

Corresponding author address: D. Jakubczyk, Institute of Physics, Polish Academy of Sciences, Al. Lotników 32/46, 02-668 Warsaw, Poland.
E-mail: jakub@ifpan.edu.pl

DOI: 10.1175/JAS3860.1

cloud droplet number concentration, and size distribution obtained with cloud models (Ackerman et al. 1995; Snider et al. 2003; Laaksonen et al. 2004; Chuang et al. 1997). For example, for $\alpha_C < 0.1$ in comparison to $\alpha_C = 1$ cloud droplet number concentration may increase by approximately 50%. These effects are generally much smaller for α_T and are usually neglected.

Many attempts have been made over nearly a century, to determine experimentally the values of α_C and α_T for water, but the results obtained by different authors spanned from ~0.001 to 1 for α_C and from ~0.5 to 1 for α_T (see, e.g., Winkler et al. 2004; Hagen et al. 1989; Zagaynow et al. 2000; Sageev et al. 1986; Gollub et al. 1974; Zou and Fukuta 1999; Shaw and Lamb 1999; Li et al. 2001; Xue et al. 2005; Marek and Straub 2001; Pruppacher and Klett 1997; Davidovits et al. 2004 for reviews). A variety of experimental methods was used. Both condensation on and evaporation from the surface of bulk liquid, liquid films, jets, and droplets were investigated in various environments (vacuum, standard, passive, or reactive atmospheres) under various pressures and for various water vapor saturations. Small droplets, such as encountered in clouds, has been favored, since large Knudsen number could be obtained even for relatively high pressure (like atmospheric pressure). Suspended droplets, trains of droplets, clouds of droplets, and single trapped droplets were studied.

There also exist theoretical considerations concerning α_C and α_T (e.g., Ward and Fang 1999; Vieceli et al. 2004; references in Marek and Straub 2001). Evaporation and condensation coefficients have been derived from the free angle ratio of water molecule, internal evaporation energy of a molecule, hole potential, and molecular dynamics simulations. Again, the results cover the range from ~0.01 to ~1. However, recent molecular dynamics simulation yield values close to 1.

The divergence of results has been usually attributed to (i) difficulties in accounting for various physical and chemical interfacial processes; (ii) effect of impurities, and especially surface active agents (Feingold and Chuang 2002; because of high molecular dipole moment, water surface is very sensitive to contamination in general); (iii) structure of the interface (dynamic surface tension, reaching the balance by the interface); and (iv) dependence of the coefficient value upon the model used (indirectness of measurement). It has been pointed out (Marek and Straub 2001; Pruppacher and Klett 1997) that two classes of experiments could be distinguished: (i) with a quasi-static interface, yielding $\alpha_C < 0.1$, and (ii) with a continuously renewing surface, yielding $\alpha_C \geq 0.1$. However, such categorization requires defining the time scale. Such scale has not been agreed yet, as well as the leading mechanism responsible for interface aging. For example, as it is mentioned in Marek and Straub (2001) stationary values of the surface tension are reached within milliseconds. This is far below the characteristic time scales of cloud droplet growth process, which lie in the range of seconds (or even minutes; Chuang et al. 1997).

The results of recently active groups (Davidovits et al. 2004) also fall into, similar categories [$\alpha_C = 0.17$ in Li et al. (2001) and 1 in Winkler et al. (2004) at 280 K], but seem not to follow the suggested categorization of Marek and Straub (2001). Experiments of both groups concerned condensation. In the experiments by Li et al. (2001) the uptake of $H_2^{17}O$ was measured at low pressure for liquid–gas contact time between 2 and 15 ms. This time is comparable to the surface tension relaxation time. In the experiments by Winkler et al. (2004) the condensation of water vapor on silver nanoparticles at low pressure (in the adiabatic expansion chamber) was measured. The evolution lasted ~50 ms, so in view of Marek and Straub (2001), the condensation coefficient similar or slightly smaller than in Li et al. (2001) should have been expected.

On the other hand, an experiment similar to Li et al. (2001), utilizing a water jet passing through tritium-labeled steam (Jamieson 1964), yielded $\alpha_C \simeq 0.001$ for corresponding liquid–gas contact time. It also yielded a dependence of α_C versus liquid–gas contact time from 10 μs to 1 s, indicating that $\alpha_C > 0.3$ could be expected for contact time in the order of microseconds, which is much shorter than surface tension relaxation.

The temperature dependence of α_C was rarely measured. Recently it was studied by Li et al. (2001), who found that α_C decrease with temperature between 257 and 280 K, and by Winkler et al. (2004), who found no temperature dependence (and also no temperature dependence of α_T) between 250 and 290 K. The comparison of their results can be found in Davidovits et al. (2004).

In this paper, the application of the method (first described in Zientara et al. 2005) of finding α_C and α_T to water in nitrogen under atmospheric pressure for various temperatures is presented. The method is based on the analysis of evaporation of a microdroplet of water in a humid environment. Nitrogen was used instead of air in order to avoid surface chemistry caused by such gases as CO_2 or SO_2. The liquid–gas contact time is in the order of seconds, which corresponds to the characteristic time scales of cloud droplet growth. This moderate time scale enabled determination of the temporal evolution of the droplet radius by analyzing the angle-resolved light scattering Mie interference pat-

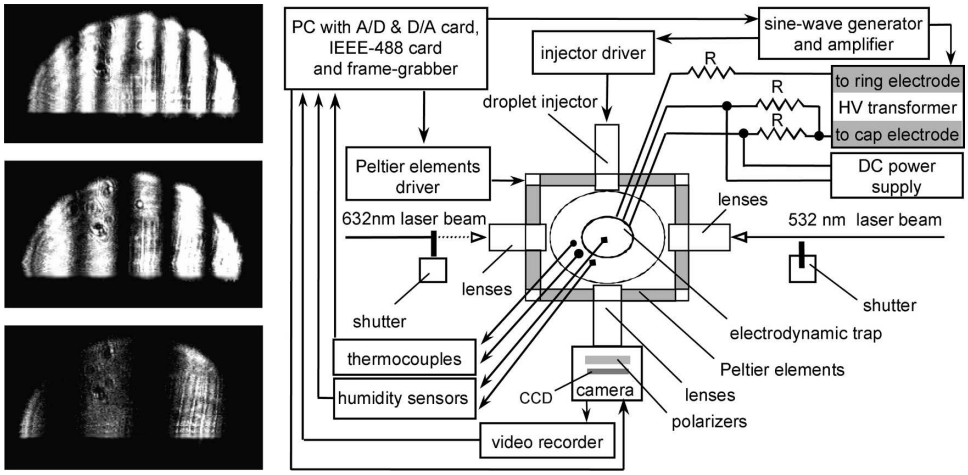

FIG. 1. (right) Experimental setup. (left) Example scatterograms (*s* polarization), corresponding to (starting from the topmost) early, middle, and late phase of an experiment for 632-nm light wavelength.

terns with high accuracy. A procedure based on Mie light scattering theory yielded evolution curves smooth enough (25 experimental points per second) to find simultaneously α_C and relative humidity S as well as α_T reliably.

2. Experiment

The experimental setup is presented in Fig. 1 and consists of an electrodynamic quadrupole trap (Paul 1990), of a hyperboloidal type, kept in a small climatic chamber. A detailed description of this apparatus can be found in Jakubczyk et al. (2001) and of further modifications in Jakubczyk et al. (2004a,b). The essential technical detail was that every electrode was driven via a 100 MΩ resistor. This was the main factor inhibiting discharges and thus enabling us to operate in a humid atmosphere.

Temperature in the upper and in the lower part of the chamber was measured (T-type thermocouple, TT-T-40-SLE, Omega) and controlled separately. Such control enabled us to eliminate vertical temperature gradients. Horizontal gradients were found to be negligible. There were also two relative humidity sensors (HIH3610–2, Honeywell): above and below the trap. The measurements of humidity performed with these sensors were rather tentative since the exchange of vapor (gas) between the interior and exterior of the utilized trap was hindered.

Before each experiment, the chamber was flushed with dry gaseous nitrogen, obtained from liquid nitrogen, in order to remove liquid water that accumulates in the chamber during experiments due to condensation and stray injection. Next, a filtered humid nitrogen (obtained by bubbling through distilled water) was passed through the chamber from the bottom to the top port. When the required humidity and a satisfactory humidity gradient were reached, the flow was stopped to enable uninfluenced, droplet trapping. Between the instants of trapping the chamber was flushed with humid nitrogen to maintain required humidity conditions.

A piezo-type droplet injector (similar to those described in, e.g., Lee and Perl 1999; Zoltan 1972) was used in the experiment. The injection timing was controlled with a digital delay circuit utilizing the trap driving AC signal zero crossing as the reference. By choosing the proper injection phase the sign and (to a certain extent) also the value of the charge deposited on the injected droplet could be controlled.

Since in our experiment the droplet injector nozzle remained at the temperature of the chamber, the initial temperature of the droplet was also the same. Since the temperature gradients across the chamber were found smaller than 0.15 K, the initial vapor density was assumed uniform across the chamber. A droplet of pure water is not in equilibrium with its surroundings for relative humidity $S \leq 1$. The fastest molecules leave the liquid phase for the vapor and thus the evaporation starts at the cost of the droplet internal energy. However, in a fraction of a second the evaporation reaches its nearly steady state (Pruppacher and Klett 1997)—the gradients of temperature and water-vapor density become nearly constant. The briefly lasting nonstationary phase could not be observed in our experiment. However it has negligible impact on further stationary process.

a. Sample preparation

Ultrapure water was produced in the laboratory in our institute (Milli-Q Plus, Millipore). A sterile plastic syringe, additionally washed with ultrapure water, was used for transferring it into the droplet injector within 10 min. The injector, made of Pyrex glass and Plexiglass, was immediately placed in the climatic chamber and the experiment was conducted within 1 h after (ultra) purification. The chemistry caused by such gases as CO_2 or SO_2 was avoided by substituting air with nitrogen in the climatic chamber.

The initial parameters of the ultrapure water used in the experiment, guaranteed by the equipment manufacturer, were: resistivity ~18 MΩcm, total dissolved solids <20 ppb, total organic carbon (TOC) ≤10 ppb, no suspended particles larger than 0.22 μm, microorganisms ≤1 colony-forming unit per milliliter, silicates <0.1 ppb, and heavy metals ≤1 ppb. Since the influence of even small amounts of surface active agents upon the experimental results might be disproportionately large, we tried to estimate it in our case. On assuming that all TOC comes from surfactants and that it is all concentrated in ~1-nm layer on the surface of the droplet, we still arrive at ~30 ppm of surfactant in this layer for a droplet of 8-μm radius (average initial radius in our experiment). If we assume that the mass of the surfactant molecule is equal to (only) 10 masses of the water molecule, than there are $\sim 3 \times 10^5$ water molecules per one surfactant molecule. During the observed evaporation droplet radius diminishes, on average, by a factor of 5, so concentration of surfactant grows by a factor of 25 (assuming that the thickness of the surface layer does not change). This yields $\sim 10^4$ water molecules per surfactant molecule for freshly purified water. Thus, the influence of surface active agents upon evaporation rate at this stage is not expected to be of importance. We were not able to determine how the water was picking up contaminants of nonionic kind during the transfer and the experiment. However, the changes of resistivity of ultrapure water loaded into the injector placed in ambient air were carefully measured and the estimate of the pickup of contaminants of ionic kind was done. It has been noticed that during the first hour after purification the concentration of such impurities grew by a factor of 3. Such an increase in concentration of ionic kinds of impurities (an 125 times increase of concentration during droplet evaporation accounted for separately) has undetectable influence upon the evolution of the droplet. If we assume, by similarity, that the concentration of surfactants grows by a factor of 3 over the same time interval, we obtain $\sim 3 \times 10^3$ water molecules per surfactant molecule (0.003 surfactant mass concentration) at the end of the evolution of the droplet. This agrees with the observed lack of droplet radius stabilization. In about 10-h time the total concentration of all dissolved substances was becoming large enough to stop the evaporation of the droplet formed of such contaminated water. At the current stage we cannot point to a specific agent responsible for this. According to the resistivity measurements described above, there would then be ~45 ppb of impurities of ionic kind in the water in the droplet injector.

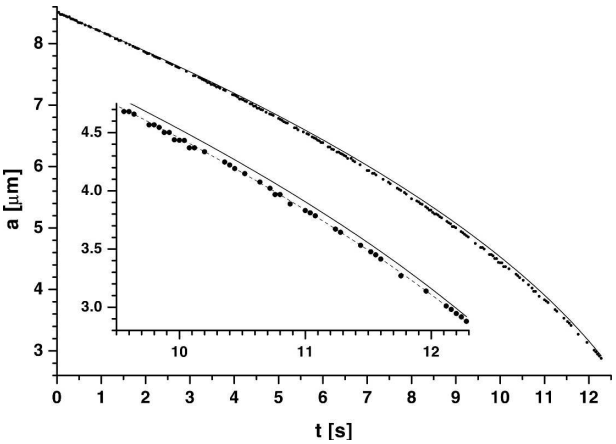

FIG. 2. An example of droplet radius evolution obtained from the experiment. Part of it magnified in the inset. Experimental conditions are $T_R = 289.1$ K, $p_{atm} = 1001.2$ hPa, relative humidity measured with sensors $S_{sens} = 89\%$. Model fits were obtained for $\alpha_C = 0.15$, $\alpha_T = 0.92$, and $S = 0.97818$ (dotted line–in the inset only) and for $\alpha_C = 0.9$, $\alpha_T = 1$, and $S = 0.97978$ (solid line). In both cases $Q = 5.8 \times 10^5$ elementary charge units correspond to Rayleigh limit reached at the end of the evolution.

b. Determination of the evolution of droplet radius

The Mie scattering interference patterns recorded during the experiment represent the scattered light irradiance I for s (vertical) polarization of the light wave, as a function of azimuth angle θ in the observation plane and elevation angle ϕ. Three example scatterograms are presented in Fig. 1. Each scattering pattern was averaged along ϕ yielding the $I(\theta)$ function. It was further smoothed by removing frequencies higher then the characteristic (distribution) from its fast Fourier transform (FFT) spectrum. The fitting of the experimental $I(\theta)$ with the theoretical $I_T(\theta)$ dependence generated with Mie formulae (see, e.g., Jakubczyk et al. 2001; Bohren and Huffman 1983) was then performed, for all video frames, and the evolution of the droplet radius $a(t)$ was found (an example in Fig. 2). The fitting was performed with a gradientless library method, where the smallest distance (L_2 measure) between the functions was sought. Besides the droplet radius a there

were two additional parameters of the fit, accounting for the movements of the droplet in the trap: effective field of view angle and the angle of side displacement. Application of this method to slowly evaporating droplet allows to find the dependence of radius upon time $a(t)$ with ± 25 nm (i.e., $\leq 1\%$) precision. However, for most rapidly evaporating droplet (for relatively lower humidities), the charge-coupled device (CCD) exposure time, for acquisition rate of 25 frames per second (fps), is comparatively long. It results in obtained pattern blur due to summation, and in turn in loss of precision up to ± 200 nm (i.e., $\leq 10\%$).

3. The model of transport of mass and heat

Many authors have discussed droplet evaporation, by also taking kinetic effects into account (see, e.g., Pruppacher and Klett 1997; Zou and Fukuta 1999; Fuchs 1959; Kozyrev and Sitnikov 2001). In our version of the model, the kinetic and surface tension effects were accounted for. The effect of droplet charge and of soluble contaminants was also incorporated (cf. e.g., Friedlander 2000; Cadle 1966), the last one for the sake of generality of the picture. Adopting a widely used model of droplet evolution enabled us to compare our results with those of other authors (see section 5). Although we concentrate on evaporation, the model considerations presented apply equally to both evaporation and condensation.

Since the temperature T_R and relative humidity S of the gas filling the reservoir was measured, it is natural to start with the equations describing the transport of heat and mass farther from the droplet, using language of diffusion. However, both theoretical and experimental studies of heat and mass transport through the gas–liquid interface indicate that there is a change of the character of flow in the very vicinity of the interface, up to the distance Δ comparable with the mean free path of particles of surrounding gaseous medium. In the region between a and $a + \Delta$ the molecules leaving or reaching the interface do not collide in average. Considering the mass and heat transport in this virtually collisionless region, resembling evaporation into the vacuum, requires using the language of kinetic theory of gases. Since the mathematical form of equations both in diffusion and kinetic regimes are similar, it is possible to write them down in the compact form. This is a widely accepted procedure that can be found, for example, in Pruppacher and Klett (1997). Thus, the steady-state evaporation of a charged droplet of diluted solution can be described with the mass (1) and heat (2) transport equations in the following form:

$$a\frac{da}{dt} \equiv a\dot{a} = \frac{MD_k(a, T_a)}{R\rho_L} \times \left\{ S\frac{p_s(T_R)}{T_R} - \frac{p_s(T_a)}{T_a} \exp \times \left[\frac{M}{RT_a\rho_L}\left(\frac{2\gamma}{a} - \frac{Q^2}{32\pi^2\varepsilon_0 a^4}\right) - n_s\frac{a_0^3}{a^3}\right]\right\}, \tag{1}$$

$$a\dot{a} = \frac{\lambda_K(a, T_a)}{q\rho_L}(T_a - T_R), \tag{2}$$

where T_a, Q, and a_0 are the droplet temperature, charge, and initial radius, respectively, p_s is the saturated vapor pressure at a given temperature, γ, ρ_L, M, and q are the surface tension, density, molecular mass, and the latent heat of evaporation of liquid water, ε_0 is the permittivity of vacuum, n_s is the concentration of soluble contaminants and R is the universal gas constant. According to Eq. (1), the evolution of the droplet mass (radius) is driven by the difference of vapor density near the droplet surface (term with exponential) and far from the droplet (in the reservoir; term with S). The terms in exponential account for the modification of vapor density near the droplet surface due to surface curvature (Kelvin term), charge effects and volume contamination effects respectively. The influence of soluble contaminants was considered within the limit of very low concentrations. The change of droplet mass by evaporation (condensation) is associated with heat absorption (release), which manifests as temperature difference between the droplet and the reservoir. The effective diffusion coefficient D_k and the effective thermal conductivity of moist nitrogen λ_K account for gas kinetic effects:

$$D_k = \frac{D}{a/(a + \Delta_C) + D\sqrt{2\pi M/(RT_a)}/(a\alpha_C)}, \tag{3}$$

$$\lambda_K = \frac{\lambda}{a/(a + \Delta_T) + \lambda\sqrt{2\pi M_N/(RT_a)}/(a\alpha_T\rho_N c_P)}, \tag{4}$$

where D is the diffusion constant for water vapor in nitrogen and λ, ρ_N, M_N, and c_P are thermal conductivity, density, molecular mass and specific heat capacity under constant pressure of (moist) nitrogen. Since for water and lower-troposphere conditions the partial pressure of water vapor can be neglected in comparison to that of nitrogen, it can be assumed that heat is conducted to the droplet mostly by the molecules of nitrogen. In consequence, the flux of mass can be considered

separately from the flux of heat and Δ_C associated with the transport of mass should be distinguished from Δ_T associated with the transport of heat.

Though the concept of charged droplet Rayleigh stability does not enter the droplet evolution model directly, Eqs. (1)–(2) must be supplemented with the Rayleigh condition (Duft et al. 2002):

$$\frac{E_Q}{2E_\gamma} = \frac{Q^2}{64\pi^2\varepsilon_0\gamma a^3} < 1, \tag{5}$$

where E_Q is the Coulomb energy of a charged droplet and E_γ is the energy associated with the surface tension. Electrically neutral, clean droplets evaporate completely. Evaporation of charged droplets may be accompanied by loss of charge and (little) mass by means of Coulomb explosions, or, for very small droplets, with loss of charge by field emission (Loscertales and de la Mora 1995; Gamero-Castaño 2002). For the droplets of a solution a stabilization of the size is possible since the increase of concentration reduces the vapor pressure over the surface of the solution. A stable droplet of finite size in nonsupersaturated vapor is possible only in the presence of contaminants.

To test the model presented above, Eqs. (1)–(2) have been solved numerically for water in nitrogen (see Fig. 3). The values of constants pertaining to water properties were taken from Pruppacher and Klett (1997), The International Association for the Properties of Water and Steam (1998, 1992, 1994), Harvey et al. (1998), Perkins et al. (1991), and Ziebland and Burton (1958), and the values of $\Delta_C = 10.4 \times 10^{-8}$ m and $\Delta_T = 2.16 \times 10^{-7}$ m were taken from Pruppacher and Klett (1997). The influence of temperature dependence of λ, ρ_L, D, γ, q, Δ_C, and Δ_T upon the solution of equations set (1)–(2), in the range of temperatures 233 K $< T_R <$ 313 K, was found to be below 0.5% and was considered negligible (The International Association for the Properties of Water and Steam 1992, 1994, 1998; Hall and Pruppacher 1976). The departure of temperature of the droplet from the temperature of the reservoir $T_a - T_R$ was found to be always well below 1 K.

4. Determination of evaporation and thermal accommodation coefficients α_C and α_T

From the experiment, the evolution of droplet radius $a(t)$ was obtained and then $a\dot{a}(t)$ was found. The analysis was restricted to the range of radii $a(t) < 8$ μm and $d^2a/dt^2 < 0$. The quantities p_{atm} and T_R come from the measurement. The evolution of droplet temperature T_a during the evaporation was then calculated from Eq. (2) within diffusion limit ($\lambda_K \to \lambda$) and inserted into the Eq. (1). Such approximation was found quite harmless. For $d^2a/dt^2 < 0$ negligence of terms corresponding to the influence of dissolved contaminants and charge is quite legitimate. Even the charge corresponding to Rayleigh limit does not influence the evolution significantly in this region. Therefore, Eq. (1) can be integrated within $\langle t_L, t_H \rangle$ limits. An algebraic equation binding α_C and S follows. If we randomly select two different $\langle t_L, t_H \rangle$ ranges (t_L and t_H should not be too close), we obtain a solvable algebraic equation set, yielding α_C and S. Repeating this procedure yields statistical distributions of α_C and S. These distributions reflect the errors in determining $a(t)$ and $\dot{a}(t)$. Both α_C and S distributions were fitted with normal distributions and the most probable value of α_C and S was taken. Half-width at half-maximum (HWHM) of the α_C distribution was taken for the uncertainty of α_C. However, the resulting coefficient value was also found to depend on the details of the data handling procedures (e.g., smoothing). The (systematic) error introduced in this way was hard to evaluate. Basing on our numerical experiments we added 50% to HWHM error limits. Having applied the whole procedure to various datasets enabled studying the dependence of α_C versus temperature. The results are presented in Fig. 4. The evaporation coefficient for the temperature range from 273.6 to 298.3 K was found to be between 0.054 and 0.12. A minimum at ~277 K was encountered, apparently coinciding with the maximum density of water. This minimum value of α_C is 0.036 ± 0.015. A dashed line in Fig. 4 represents a best

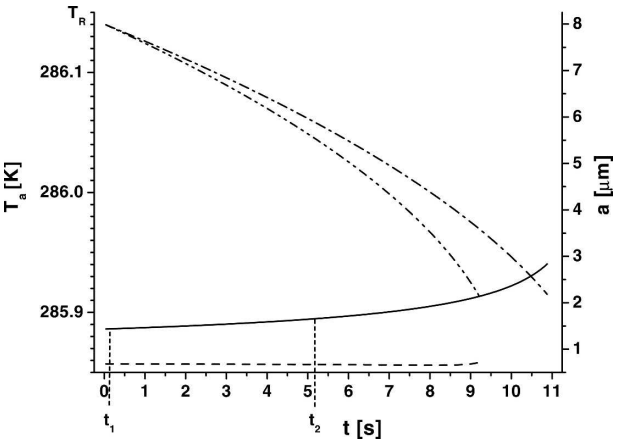

FIG. 3. Numerical simulation of the evolution of water droplet radius (dash–dot and dash–dot–dot lines) and of droplet temperature (solid and dashed lines). Dashed and dash–dot–dotted lines represent kinetic effects not accounted for in Eqs. (1) and (2); solid and dash–dotted lines represent complete formulas. Evolution terminates with Coulomb explosion at $a = 2155$ nm; $T_a(t)$ can be linearly approximated between t_1 and t_2. Model parameters are $p_{\text{atm}} = 1001.2$ hPa, $T_R = 286.15$ K, $a_0 = 8$ μm, $Q = 4 \times 10^5$ elementary charge units, $n_s = 0$, $S = 0.97$, $\alpha_C = 0.07$, and $\alpha_T = 0.7$.

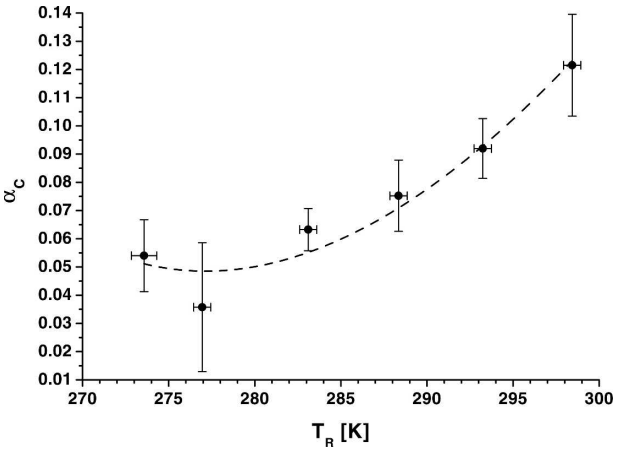

FIG. 4. Evaporation coefficient of water in nitrogen under atmospheric pressure vs reservoir temperature. The dashed line represents a function inversely proportional to the density of water.

fit based on an assumption that the evaporation coefficient is inversely proportional to density of liquid water to the power of *d:* $\alpha_C \sim (1/\rho_L)^d$. However we could not find the value of d unambiguously (surface density $\rho_L^{-2/3}$ would be the first guess). Qualitatively similar results were obtained for water in air for the same temperature range, as should have been expected because of the high nitrogen content in air (cf. Zientara et al. 2005).

Having found α_C and S enabled proceeding to α_T. It can be noted (see Fig. 2), that for steady-state evaporation, for the range of time $t_1 < t < t_2$, $T_a(t)$ can be treated as a linear function of time. Equation (2) can then be written down in the following form:

$$Bt + C = T_R + a\dot{a}\,\frac{q\rho_L}{\lambda_K}, \tag{6}$$

where B and C are constants. By writing down the Eq. (6) for three randomly chosen points in time in the range $\langle t_1, t_2\rangle$ (the points should not be too close), we obtain a solvable equation set and find B, C and α_T (by finding λ_K). We restrict ourselves to solutions, where $A > 0$, $B > 0$, and $0 < \alpha_T < 1$. Repeating this procedure yields a statistical distribution of α_T. This distribution was fitted with a normal distribution and the most probable value of α_T was taken. Again, HWHM of this distribution plus 50% was taken for the uncertainty of α_T. However, this procedure is essentially approximate and also extremely sensitive to $\dot{a}a$ inaccuracy. Because of limited quality of the experimental data, the temperature dependence of α_T could not be characterized and only its average value in the temperature range from 277 to 289 K could be given: 0.7 ± 0.2. This is in agreement with the previous result for water in air (Zientara et al. 2005).

5. Discussion

The presented values of mass and thermal accommodation coefficients are not direct experimental numbers but depend on the underlying model. We used a frequently utilized model of droplet evolution, so the results can be compared with other authors. A few issues pertaining to the approximations made have already been discussed. However, we would like to address some others.

(i) The velocity distribution in the very vicinity of an evaporating droplet may be non-Maxwellian and the mean velocities of vapor and gas molecules entering into expressions (3) and (4) may not be fully justified.

(ii) The matching of gas kinetic and diffusional regime is an essential part of the model applied. However, a molecule-free path may differ considerably from a mean free path, which smears the concept of a matching point and makes Δ_T and Δ_C much arbitrary parameters. Indeed, having changed Δ_T by a factor of up to 4 or Δ_C by a factor of up to 40, had a negligible effect upon the evolution of $a(t)$ or $T(t)$.

(iii) Using Kelvin formula for expressing vapor density near the curved, charged surface is not fully justified for a nonstationary state. It seems more appropriate to introduce the effects of surface curvature and charge into the latent heat of evaporation, which is ordinarily defined for a flat, neutral surface. However this would considerably change the model and would result in changes of α_C and α_T. We intend to study this problem further.

(iv) There are many constants (taken from the literature) and parameters of the model that are known with finite accuracy. This might influence the accuracy of finding α_C and α_T. However, it has been found that the accuracy of determining droplet radius has, mainly through the action of derivative, a much greater impact upon the accuracy of α_C and α_T than any other constant or parameter. The accuracy of measuring the temperature and pressure of droplet surroundings has negligible impact upon the accuracy of α_C and α_T but weights upon S. Apart from that, the direct fitting of the model to the experimental data seems to suggest that the accuracy of temperature measurements is better (± 0.2 K) than guaranteed by the thermocouple manufacturer.

As has been mentioned in the introduction, the value of mass accommodation coefficient depends on the state of the interface. For water (and also for other liquids) it has been reported to decrease after the interface formation by ~3 orders of magnitude for the time span from microseconds to seconds (Jamieson 1964; Marek and Straub 2001). There seem to be a few processes involved (molecules orientation, dynamic surface tension, gas adsorption by dipole forces). This raises a few issues: What is the normal state of the interface? For different liquids different processes may participate in interface stabilization—which of them should be accounted for separately while measuring the accommodation coefficient? We have adhered to the following attitude: The accommodation coefficients have been traditionally introduced for (quasi) stationary processes, and a great care is required in applying them to fast processes. All the processes occurring at time scales much shorter than seconds should be included in the value of the accommodation coefficient. Accommodation coefficients defined in such way can be applicable to microphysical processes in clouds.

Our analysis of the experimental data seems to indicate that another source of spread of results may prevail in many cases. It is well known that the α_C value is very sensitive to relative humidity (Chuang et al. 1997; Kulmala et al. 2001; Zientara et al. 2005). Here α_C and S partially overlap [see Eqs. (1) and (3)]. For relative humidities close to unity (above or below) changes below 1% in S (which are instrumentally unmeasurable) cause dramatic changes in α_C. If S is taken from the measurement and α_C is calculated (fitted) from droplet evolution data, a large error in α_C may easily happen. In our work we overcome this problem by fitting simultaneously S and α_C. We illustrate this issue in Fig. 3. The experimentally obtained droplet radius evolution (solid circles) is precisely reconstructed with model predictions for $\alpha_C = 0.15$, $\alpha_T = 0.92$, and $S = 0.97818$ (dotted line). However, for $\alpha_C = 0.9$ and $\alpha_T = 1$ the best fit is for $S = 0.97978$ (solid line), which is well below any instrumental S measurement resolution. The fit curves are shifted by less than 100 nm, and for even slightly less precise method of droplet radius measurement, they would be statistically undistinguishable. It must be noted, that the value of S found by fitting is, to a certain extent, a parameter of fit. Its absolute accuracy is limited by the accuracy of temperature T_R measurement.

6. Conclusions

The temperature dependence of evaporation coefficient α_C and thermal accommodation coefficient α_T was studied for water in gaseous nitrogen at atmospheric pressure. The dynamics of the evolution of radius of the evaporating levitated droplet was studied. The time scale of the process in the region of seconds corresponds to droplet growth time in clouds. A very precise, laser light scattering method was used to study the droplet evolution. The interference scattering patterns were analyzed with electromagnetic Mie scattering theory. The precision of the method enabled simultaneous finding of evaporation coefficient and relative humidity, and avoiding errors introduced by instrumental humidity measurement. Results for both evaporation and thermal accommodation coefficients α_C and α_T were obtained similar to those of, for example, Hagen et al. (1989), Zagaynow et al. (2000), Shaw and Lamb (1999), and Li et al. (2001). The investigation suggests that there is a temperature dependence of evaporation coefficient, possibly exhibiting a minimum coinciding with the maximum density of water. This temperature dependence is different than obtained by other authors (Li et al. 2001; Winkler et al. 2004). A possibility of finding thermal accommodation coefficient simultaneously with evaporation coefficient (Zientara et al. 2005) was confirmed.

Acknowledgments. This work was supported by Polish Ministry of Education and Science Grant 1 P03B 117 29.

REFERENCES

Ackerman, A., O. Toon, and P. Hobbs, 1995: A model for particle microphysics, turbulent mixing, and radiative transfer in the stratocumulus-topped marine boundary layer and comparisons with measurements. *J. Atmos. Sci.,* **52,** 1204–1236.

Bohren, C., and D. Huffman, 1983: *Absorption and Scattering of Light by Small Particles.* Wiley, 530 pp.

Cadle, R., 1966: *Particles in the Atmosphere and Space.* Reinhold, 226 pp.

Chuang, P., R. Charlson, and J. Seinfeld, 1997: Kinetic limitations on droplet formation in clouds. *Nature,* **390,** 594–596.

Davidovits, P., and Coauthors, 2004: Mass accommodation coefficient of water vapor on liquid water. *Geophys. Res. Lett.,* **31,** L22111, doi:10.1029/2004GL020835.

Duft, D., H. Lebius, B. Huber, C. Guet, and T. Leisner, 2002: Shape oscillations and stability of charged microdroplets. *Phys. Rev. Lett.,* **89,** doi:10.1103/PhysRevLett.89.084503.

Feingold, G., and P. Chuang, 2002: Analysis of the influence of film-forming compounds on droplet growth: Implications for cloud microphysical processes and climate. *J. Atmos. Sci.,* **59,** 2006–2018.

Friedlander, S., 2000: *Smoke, Dust, and Haze: Fundamentals of Aerosol Dynamics.* Oxford University Press, 407 pp.

Fuchs, N., 1959: *Evaporation and Droplet Growth in Gaseous Media.* Pergamon Press, 72 pp.

Gamero-Castaño, M., 2002: Electric-field-induced ion evaporation from dielectric liquid. *Phys. Rev. Lett.,* **89,** doi:10.1103/PhysRevLett.89.147602.

Gollub, J., I. Chabay, and W. Flygare, 1974: Laser heterodyne study of water droplet growth. *J. Chem. Phys.,* **61,** 2139–2144.

Grimm, R., and J. Beauchamp, 2002: Evaporation and discharge dynamics of highly charged droplets of heptane, octane, and p-xylene generated by electrospray ionization. *Anal. Chem.,* **74,** 6291–6297.

Hagen, D., J. Schmitt, M. Trublood, J. Carstens, D. White, and D. Alofs, 1989: Condensation coefficient measurement for water in the UMR cloud simulation chamber. *J. Atmos. Sci.,* **46,** 803–816.

Hall, W., and H. Pruppacher, 1976: The survival of ice particles falling from cirrus clouds in subsaturated air. *J. Atmos. Sci.,* **33,** 1995–2006.

Harvey, A., J. Gallagher, and J. Levelt Sangers, 1998: Revised formulation for the refractive index of water and steam as function of wavelength, temperature and density. *J. Phys. Chem. Ref. Data,* **27,** 761–775.

International Association for the Properties of Water and Steam, 1992: Revised supplementary release on saturation properties of ordinary water substance. IAPWS Tech. Rep., 7 pp.

——, 1994: IAPWS release on surface tension of ordinary water substance. IAPWS Tech. Rep., 4 pp.

——, 1998: Revised release on the IAPS formulation 1985 for the thermal conductivity of ordinary water substance. IAPWS Tech. Rep., 23 pp.

Jakubczyk, D., M. Zientara, W. Bazhan, M. Kolwas, and K. Kolwas, 2001: A device for light scatterometry on single levitated droplets. *Opto-Electron. Rev.,* **9,** 423–430.

——, G. Derkachov, W. Bazhan, E. Łusakowska, K. Kolwas, and M. Kolwas, 2004a: Study of microscopic properties of water fullerene suspensions by means of resonant light scattering analysis. *J. Phys.,* **37D,** 2918–2924.

——, ——, M. Zientara, M. Kolwas, and K. Kolwas, 2004b: Local-field resonance in light scattering by a single water droplet with spherical dielectric inclusions. *J. Opt. Soc. Amer.,* **21A,** 2320–2323.

Jamieson, D., 1964: Condensation coefficient of water. *Nature,* **202,** 583.

Kozyrev, A., and A. Sitnikov, 2001: Evaporation of a spherical drop in a middle pressure gas. *Usp. Fiz. Nauk,* **171,** 765–774.

Kulmala, M., A. Lauri, H. Vehkamalki, A. Laaksonen, D. Petersen, and P. Wagner, 2001: Strange predictions by binary heterogeneous nucleation theory compared with a quantitative experiment. *J. Phys. Chem.,* **105B,** 11 800–11 808.

Laaksonen, A., T. Vesala, M. Kulmala, P. Winkler, and P. Wagner, 2004: On cloud modelling and the mass accommodation coefficient of water. *Atmos. Chem. Phys. Discuss.,* **4,** 7281–7290.

Lee, E., and M. Perl, 1999: Universal fluid droplet ejector. U.S. Patent No. 5943075. [Available online at http://www.uspto.gov/patft/index.html.]

Li, Y., P. Davidovits, Q. Shi, J. Jayne, C. Kolb, and D. Worsnop, 2001: Mass and thermal accommodation coefficients of H_2O (g) on liquid water as function of temperature. *J. Phys. Chem.,* **105A,** 10 627–10 634.

Loscertales, I., and J. de la Mora, 1995: Experiments on the kinetics of field evaporation of small ions from droplets. *J. Chem. Phys.,* **103,** 5041–5060.

Marek, R., and J. Straub, 2001: Analysis of the evaporation coefficient and the condensation coefficient of water. *Int. J. Heat Mass Transfer,* **44,** 39–53.

McFiggans, G., and Coauthors, 2005: The effect of physical and chemical aerosol properties on warm cloud droplet activation. *Atmos. Chem. Phys. Discuss.,* **5,** 8507–8646.

Paul, W., 1990: Electromagnetic traps for charged and neutral particles. *Rev. Mod. Phys.,* **62,** 531–540.

Perkins, R., H. Roder, D. Friend, and C. Nieto de Castro, 1991: The thermal conductivity and heat capacity of fluid nitrogen. *Physica A,* **173,** 332–362.

Pruppacher, H., and J. Klett, 1997: *Microphysics of Clouds and Precipitation.* Kluwer Academic, 954 pp.

Sageev, G., R. Flagan, J. Seinfeld, and S. Arnold, 1986: Condensation of water on aqueous droplets in the transition regime. *Colloid Interface Sci.,* **113,** 421–429.

Sazhin, S., 2005: Modelling of heating, evaporation and ignition of fuel droplets: Combined analytical, asymptotic and numerical analysis. *J. Phys. Conf. Ser.,* **22,** 174–193.

Shaw, R., and D. Lamb, 1999: Experimental determination of the thermal accommodation and condensation coefficients of water. *J. Chem. Phys.,* **111,** 10 659–10 663.

Shi, Q., P. Davidovits, J. Jayne, D. Worsnop, and C. Kolb, 1999: Uptake of gas-phase ammonia. 1: Uptake by aqueous surfaces as a function of pH. *J. Phys. Chem.,* **103A,** 8812–8823.

Snider, J., S. Guibert, J.-L. Brenguier, and J.-P. Putaud, 2003: Aerosol activation in marine stratocumulus clouds. 2: Köhler and parcel theory closure studies. *J. Geophys. Res.,* **108,** 8629, doi:10.1029/2002JD002692.

Vieceli, J., M. Roeselová, and D. Tobias, 2004: Accommodation coefficients for water vapor at the air/water interface. *Chem. Phys. Lett.,* **393,** 249–255.

Ward, C., and G. Fang, 1999: Expression for predicting liquid evaporation flux: Statistical rate theory approach. *Phys. Rev. E,* **59,** 429–440.

Winkler, P., A. Vrtala, P. Wagner, M. Kulmala, K. Lehtinen, and T. Vesala, 2004: Mass and thermal accommodation during gas–liquid condensation of water. *Phys. Rev. Lett.,* **93,** 07 570, doi:10.1103/PhysRevLett.93.075701.

Xue, H., A. Moyle, N. Magee, J. Harrington, and D. Lamb, 2005: Experimental studies of droplet evaporation kinetics: Validation of models for binary and ternary aqueous solutions. *J. Atmos. Sci.,* **62,** 4310–4326.

Zagaynow, V., V. Nuzhny, T. Cheeusova, and A. Lushnikov, 2000: Evaporation of water droplet and condensation coefficient: Theory and experiment. *J. Aerosol Sci.,* **31** (Suppl. 1), S795–S796.

Ziebland, H., and J. Burton, 1958: The thermal conductivity of nitrogen and argon in the liquid and gaseous state. *Br. J. Appl. Phys.,* **9,** 52–59.

Zientara, M., D. Jakubczyk, G. Derkachov, K. Kolwas, and M. Kolwas, 2005: Simultaneous determination of mass and thermal accommodation coefficients from temporal evolution of an evaporating water microdroplet. *J. Phys.,* **38D,** 1978–1983.

Zoltan, S., 1972: Pulsed droplet ejecting system. U.S. Patent No. 3683212. [Available online at http://www.uspto.gov/patft/index.html.]

Zou, Y., and N. Fukuta, 1999: The effect of diffusion kinetics on the supersaturation in clouds. *Atmos. Res.,* **52,** 115–141.